

Low-Level Detection of Water in Polar Aprotic Solvents Using an Unusually Fluorescent Spirocyclic Rhodamine

Palani Yuvaraj,^{ab} Joseph Ajantha,^{ab} Shanmugam Easwaramoorthi,^{*a} and Jonnalagadda
Raghava Rao^{*a}

^a, Inorganic & Physical Chemistry Laboratory, CSIR-Central Leather Research Institute, Adyar 600 020, India

^b, University of Madras, Chepauk, Chennai – 600005, India

S1. Experimental section

The detailed synthetic route of prepared rhodamine derivatives shown clearly in Scheme S1 and S2. The product structure was confirmed by ^1H , ^{13}C , DEPT 135 NMR and ESI-MS (Fig S10 to S17). Density functional theory (DFT) calculations in a gas phase were performed using Gaussian 03 at the B3LYP/6-31G level further support the electronic properties of DRh and MRh are shown in, Figure S5 and S6.

1.1 Materials

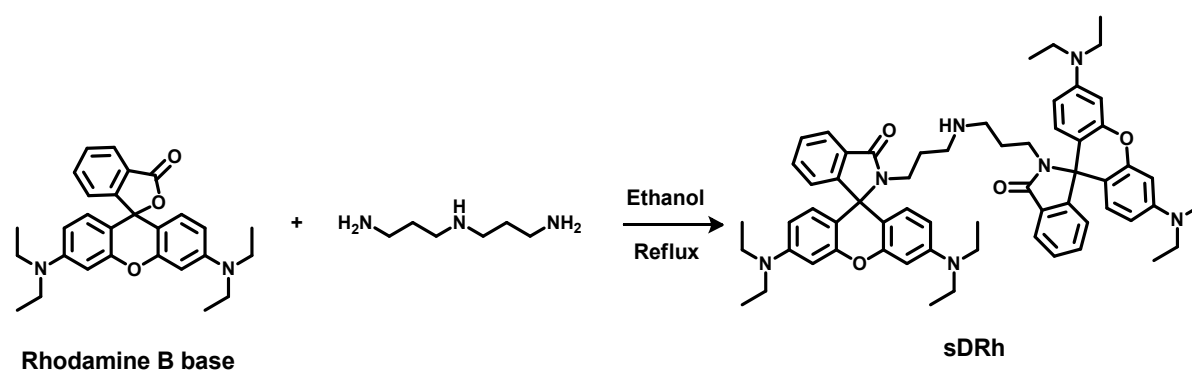
Rhodamine B base (97%), Bis(3-aminopropyl)amine (98%), 3-(methylamino)propylamine (97%) and Piperidine (97%) were obtained from Sigma-Aldrich. Ethanol (100%) was purchased from Hayman. Sodium sulphide anhydrous and all other organic solvents were HPLC grade obtained from Merck. Double distilled water is used throughout the work.

1.2 Instrumentation

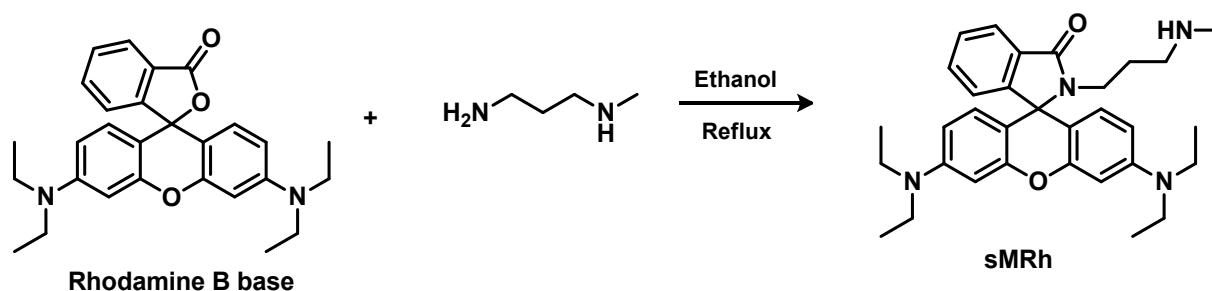
^1H and ^{13}C NMR spectra were recorded using Bruker 400 MHz and 101 MHz spectrometer respectively. Chemical shifts (δ) values were reported in ppm relative to a Tetramethylsilane (TMS) standard in CDCl_3 or THF- d_8 . ESI-MS spectra were recorded using LCQ advantage max Thermofisher instruments. UV-Vis absorption studies were done by using SHIMADZU 1800 spectrophotometer. The fluorescence spectra were collected by using Varian Cary Eclipse fluorescence spectrophotometer. Time-Correlated Single-Photon Counting (TCSPC) fluorescence lifetime was measured using Edinberg Instruments FLS980 spectrophotometer with the excitation source of 371 nm picosecond pulsed diode laser. Lifetime data analysis reconvolution fit analysis software (FLS980, Edinburgh Instruments) was used. The fluorescence quantum yield (Φ_f) of the derivative in different solvents were determined by the standard method using 0.1 M H_2SO_4 quinine sulfate as a reference sample.

Synthetic Scheme

Scheme S1. Synthesis of sDRh



Scheme S2. Synthesis of sMRh



Synthesis of sDRh

To a stirring solution of rhodamine B base (0.5 g, 1.13 mmol 2 equivalence) in absolute ethanol (30 ml), bis(3-aminopropyl)amine (79 μ l, 0.565 mmol, 1 equivalence) in ethanol (5 ml) was added and allowed to stir under reflux (85 °C) for 72 h until the pink colour of the solution changes to pale orange. The reaction mixture was then cooled to room temperature, and the ethanol was removed under reduced pressure. DCM (30 ml) was added to the orange solid and washed with water (100 ml) for three times. After drying over anhydrous sodium sulphate, the DCM solution was evaporated under reduced pressure to obtain a pale orange solid, which was further purified by DCM and hexane extraction and dried to get **sDRh**. Yield: 76.7%. m.p. 225.2 °C. ¹H NMR (400 MHz, Chloroform-*d*) δ 7.95 – 7.81 (m, 2H), 7.45 – 7.37 (m, 4H), 7.09 – 7.00 (m, 2H), 6.41 (s, 2H), 6.38 (s, 2H), 6.35 (d, $J = 2.6$ Hz, 4H), 6.23 (dd, $J = 8.9, 2.6$ Hz, 4H), 3.30 (q, $J = 7.0$ Hz, 16H), 3.09 (t, $J = 7.3$ Hz, 4H), 2.20 (t, $J = 7.2$ Hz, 4H), 1.26 (d, $J = 7.8$ Hz, 4H), 1.14 (t, $J = 7.0$ Hz, 25H). ¹³C NMR (101 MHz, Chloroform-*d*) δ 153.27, 148.70, 132.15, 128.87, 127.86, 123.69, 122.66, 107.98, 105.75, 97.68, 64.88, 47.01, 44.32, 38.22, 122.68, 107.99, 97.68, 12.63. ESI-MS: calculated for C₆₂H₇₃N₇O₄ [M+H]⁺ 981.29, found 980.62

Synthesis of sMRh

To a stirring solution of rhodamine B base (0.5 g, 1.13 mmol 2 equivalence) in absolute ethanol (30 ml), excess of N-methyl-1,3-propanediamine (0.354 ml, 3.389 mmol, 3 equivalence) in ethanol (5 ml) was added and allowed to stir under reflux (85 °C) for 48 h until the pink colour of the solution changes to orange. The reaction mixture was then cooled to room temperature, and the ethanol was removed under reduced pressure. DCM (30 ml) was added to the orange solid and washed with water (100 ml) for three times. After drying over

anhydrous sodium sulphate, the DCM solution was evaporated under reduced pressure to obtain a reddish orange solid, which was further purified by DCM and hexane extraction and dried to get **sMRh**. Yield: 80.3%. m.p. 139.3 °C. ¹H NMR (400 MHz, Chloroform-*d*) δ 7.96 – 7.84 (m, 1H), 7.48 – 7.38 (m, 2H), 7.13 – 7.04 (m, 1H), 6.48 – 6.34 (m, 4H), 6.26 (dd, *J* = 8.9, 2.6 Hz, 2H), 3.33 (q, *J* = 7.1 Hz, 8H), 3.18 (t, *J* = 7.2 Hz, 2H), 2.35 (t, *J* = 6.8 Hz, 2H), 1.31 (t, *J* = 7.0 Hz, 2H), 1.16 (t, *J* = 7.0 Hz, 13H). ¹³C NMR (101 MHz, Chloroform-*d*) δ 168.25, 153.56, 153.34, 148.77, 132.28, 131.32, 128.89, 127.98, 123.76, 122.68, 108.02, 105.75, 97.71, 64.96, 49.03, 44.35, 37.83, 36.12, 28.13, 12.59. ¹³C DEPT NMR (101 MHz, Chloroform-*d*) δ 132.29, 128.89, 127.98, 123.76, 122.68, 108.01, 97.70, 36.13, 12.59. ESI-MS: calculated for C₃₂H₄₀N₄O₂ [M+H]⁺ 513.69, found 513.25 m/z.

Lippert-Mataga method

The difference in solvent dipole moments among the ground and excited states ($\Delta\mu$) is calculated by using the Lippert–Mataga equation (eq S1)¹

$$\Delta\nu = \nu_a - \nu_f = \frac{1}{4\pi\epsilon_0} \frac{2\Delta\mu^2}{hca^3} \Delta f + constant \quad (S1)$$

where $\Delta\nu$ is the Stokes shift (cm⁻¹); ν_a and ν_f are absorption and emission maxima in wavenumber respectively; ϵ_0 is the dielectric constant of vacuum, h is the Plank constant, c is the velocity of light, a is the radius of the Onsager cavity, and Δf is the orientation polarizability of the solvent defined as follows (eq S2):

$$\Delta f = \frac{\epsilon - 1}{2\epsilon + 1} - \frac{n^2 - 1}{2n^2 + 1} \quad (S2)$$

where ϵ is the dielectric constant and n is the refractive index of the solvent.

Scheme S3.

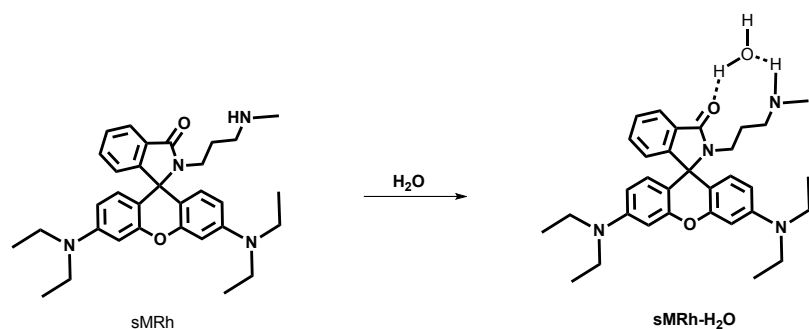


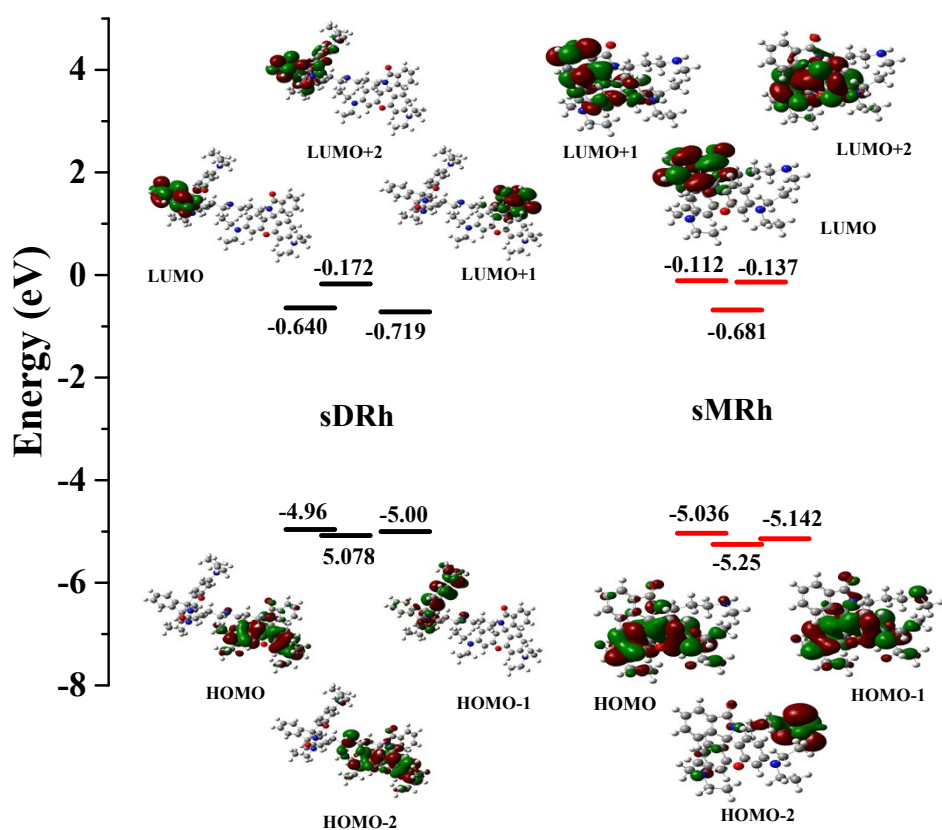
Table S1. Photophysical and photochemical data of sDRh in different solvents

Solvents	λ_{abs} (nm)	λ_{f} (nm)	$\Delta\bar{\nu}$ (cm ⁻¹)	\square_{f}	τ_1 (ns) (Rel %)	τ_2 (ns) (Rel %)
Toluene	314	408	7330	0.032	0.66 (58)	2.88 (42)
Dioxane	312	419	8180	0.076	1.02 (44)	3.75 (56)
THF	312	428	8690	0.107	1.36 (49)	3.97 (51)
EA	312	428	8690	0.068	1.19 (39)	3.76 (61)
CHCl ₃	316	439, 554	8870	0.038	1.60 (44)	4.63 (56)
DCM	316	454, 551	9620	0.069	1.37 (39)	4.37 (61)
DMF	316	473	9520	0.045	1.81 (34)	4.20 (66)
DMSO	317	491	10400	0.094	1.62 (34)	4.48 (66)
ACN	314	484	11690	0.041	1.70 (35)	4.43 (65)
2-Prop	312	489, 556	11440	0.085	1.55 (34)	4.34 (66)
EtOH	313	505, 564	12250	0.033	2.82 (94)	7.49 (6)
MeOH	314	508, 567	12260	0.011	2.32 (92)	5.76 (8)

Table S2. Photophysical and photochemical data of sMRh in different solvents

Solvents	λ_{abs} (nm)	λ_{f} (nm)	$\Delta\bar{\nu}$ (cm ⁻¹)	\square_{f}	τ_1 (ns) (Rel %)	$\tau_{2\text{f}}$ (ns) (Rel %)
Toluene	313	406	7320	0.033	0.62 (51)	2.73 (49)
Dioxane	312	415	7960	0.087	0.77 (41)	3.49 (59)
THF	313	431	8750	0.109	1.19 (65)	3.60 (65)
EA	314	430	8590	0.071	1.01 (30)	3.42 (70)
CHCl ₃	316	446, 525	9220	0.040	1.48 (38)	4.44 (62)
DCM	317	455	9570	0.088	1.38 (34)	4.37 (66)
DMF	316	474	10550	0.069	1.68 (35)	4.43 (65)
DMSO	317	489	11100	0.125	1.23 (42)	4.57 (56)
ACN	314	489	11500	0.025	1.49 (28)	4.31 (72)
2-Prop	312	486, 528	11480	0.075	1.71 (37)	4.78 (63)
EtOH	313	503, 532	12070	0.018	2.21 (29)	4.34 (71)
MeOH	313	504, 542	12110	0.005	2.33 (34)	4.30 (66)

Figure S1. DFT energy level diagram and relative isosurfaces of sDRh and sMRh, HOMO and LUMO levels.



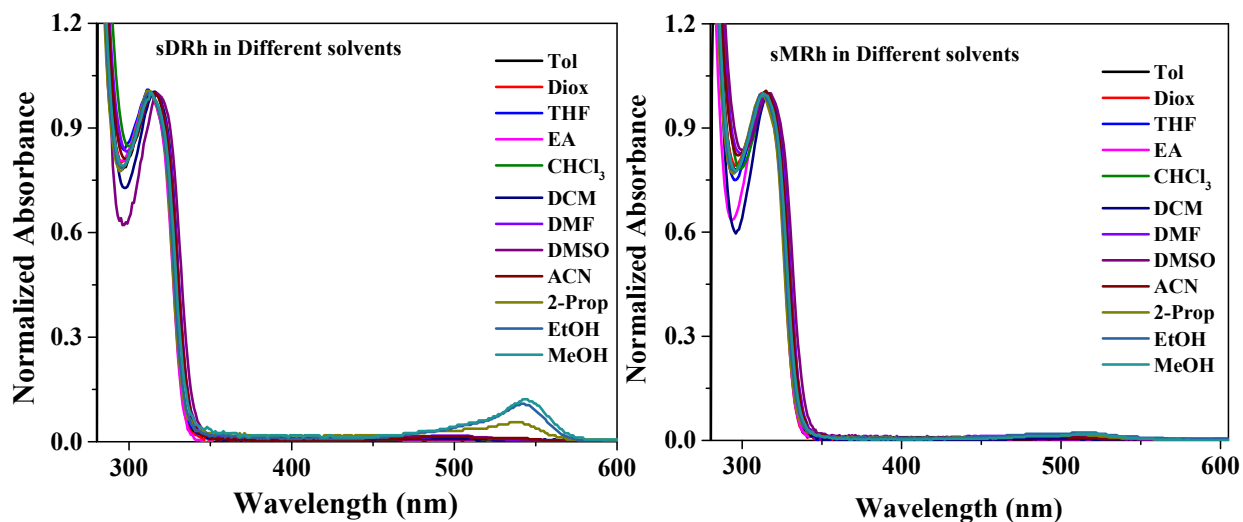


Figure S2. Absorption Spectrum of DRh and MRh in different solvents

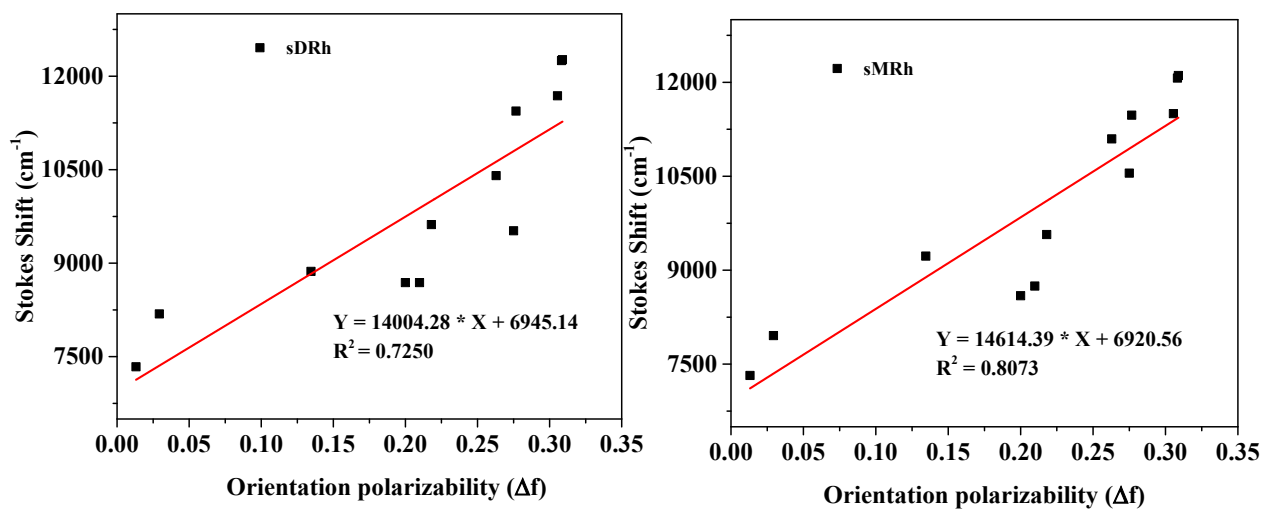


Figure S3. Lippert-Mataga Correlation of Stokes shift in wavenumber ($\Delta\nu$) vs the orientational polarizability (Δf)

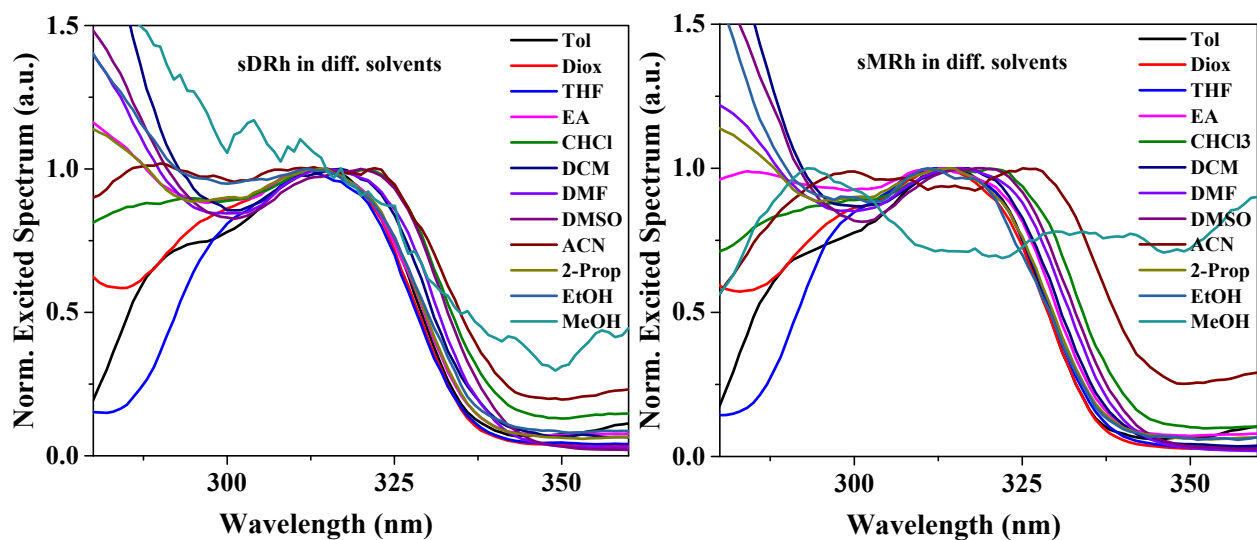


Figure S4. Excited Spectrum of sDRh and sMRh in different solvents

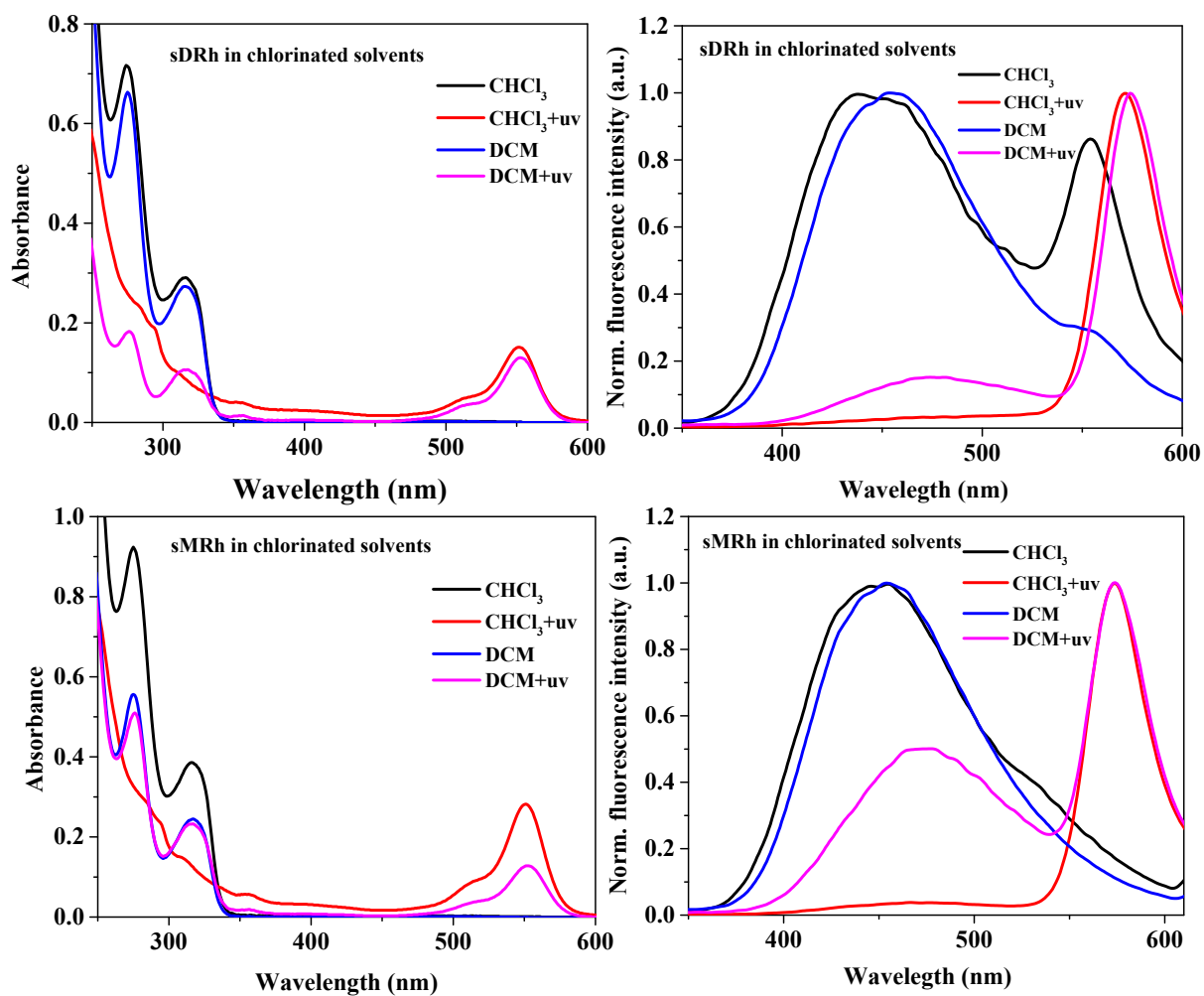


Figure S5. Absorption and emission spectrum of sDRh and sMRh before and after uv irradiation in Chlorinated solvents (Chloroform and Dichloromethane)

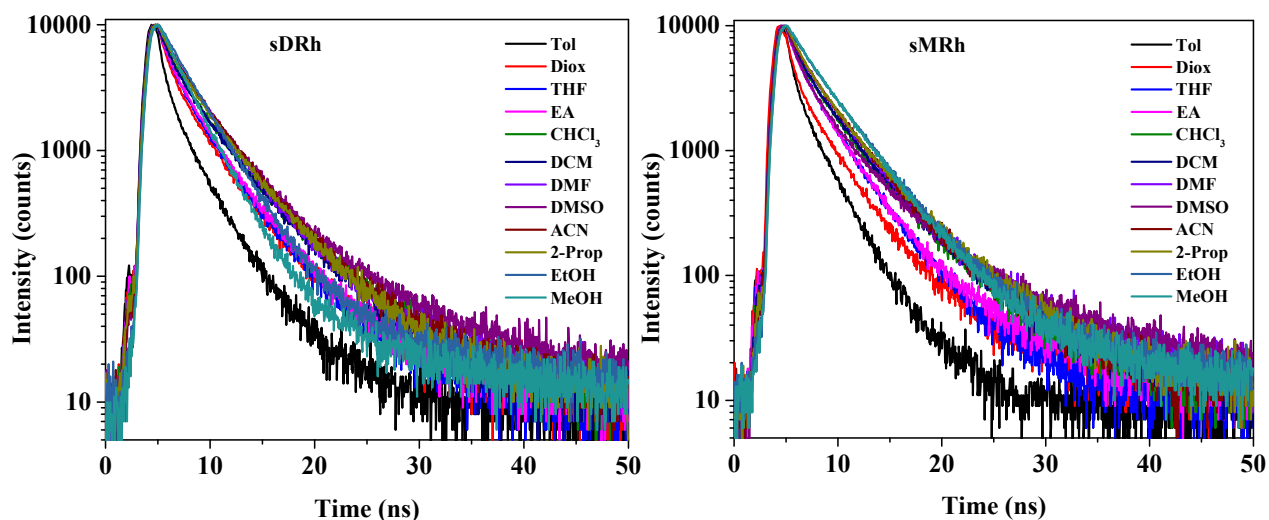


Figure S6. Fluorescence decay profile of sDRh and sMRh in different solvents.

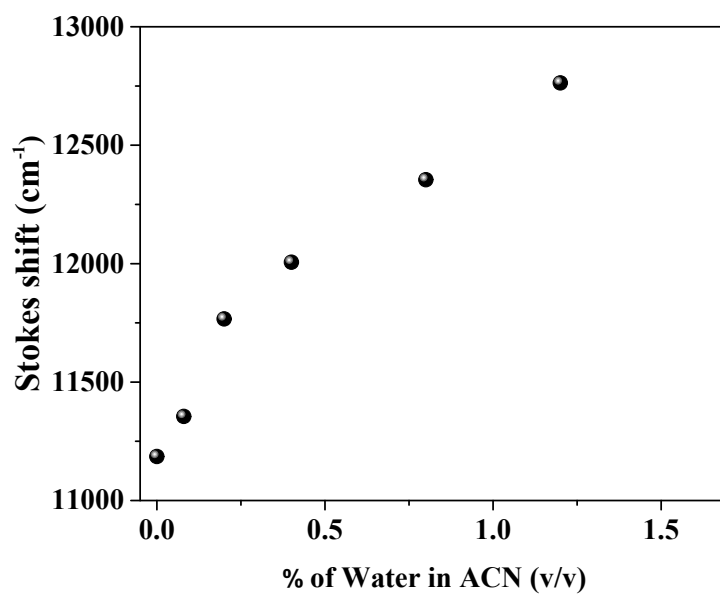


Figure S7. Correlation between stoke's shift and % of water in acetonitrile

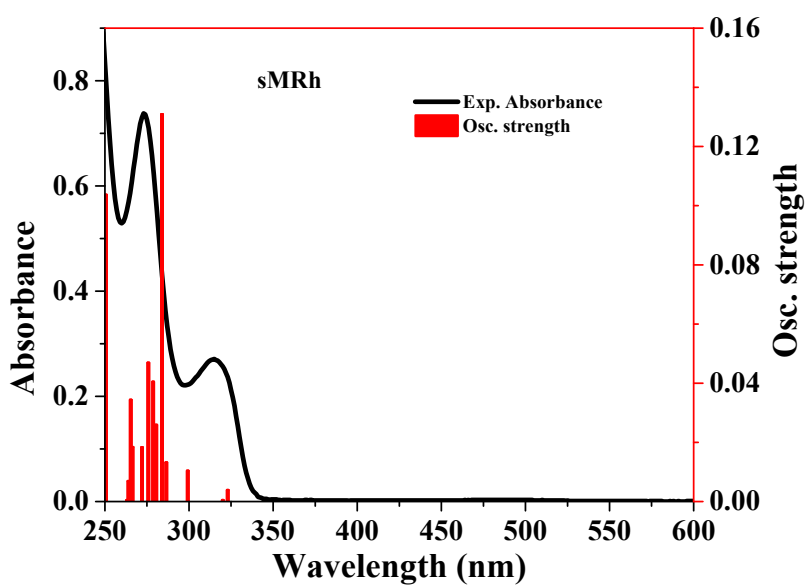
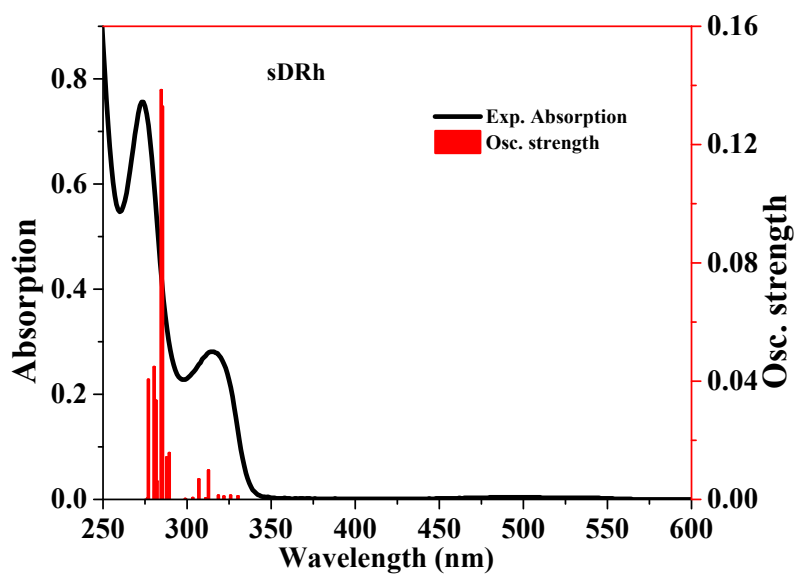


Figure S8. An overlay of the experimental absorption spectrum and DFT calculated oscillator strengths of sDRh and sMRh

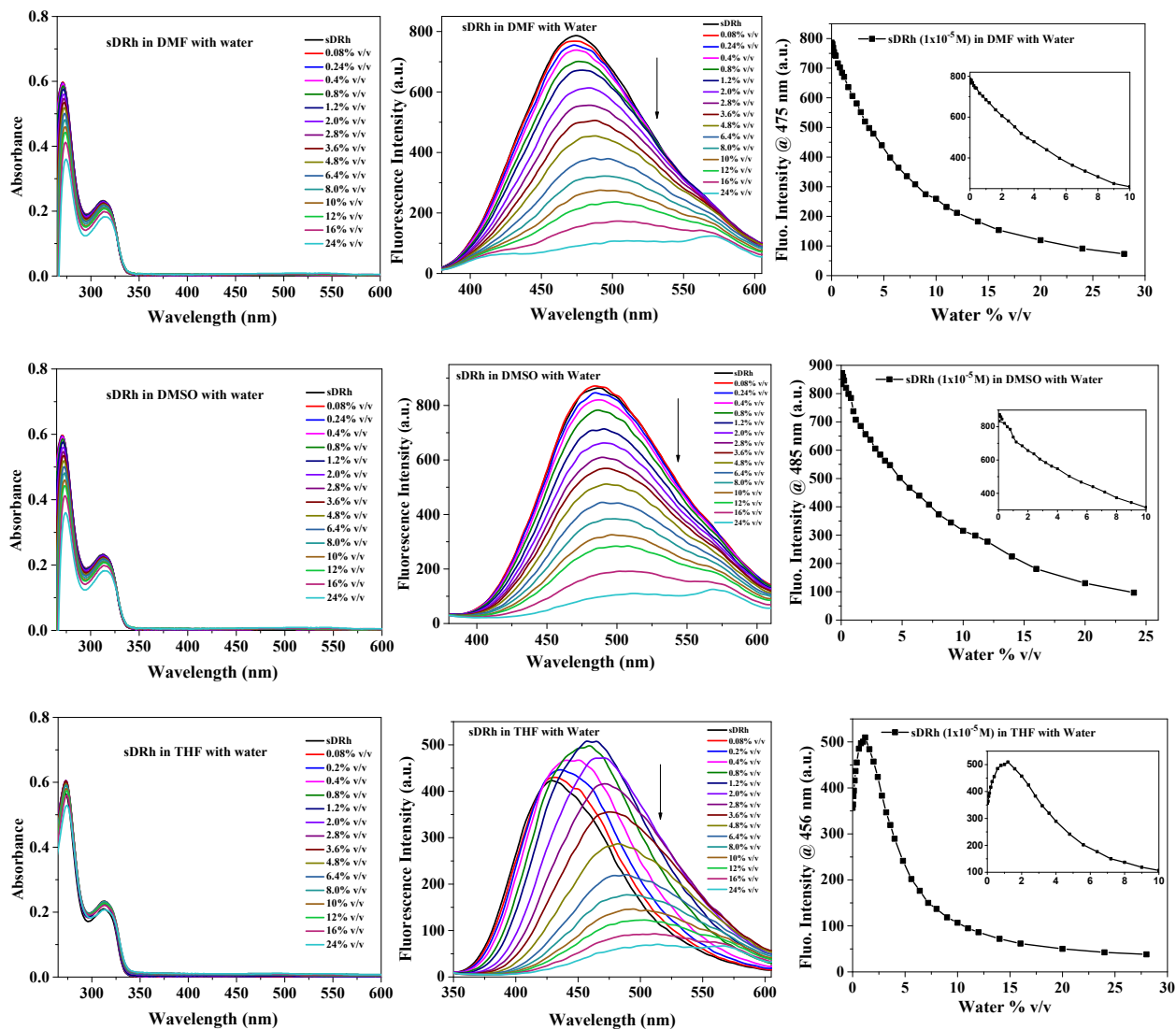


Figure S9. Fluorescence spectrum and fluorescence emission intensity of the sDRh as a function of the water content in DMF , DMSO and THF.

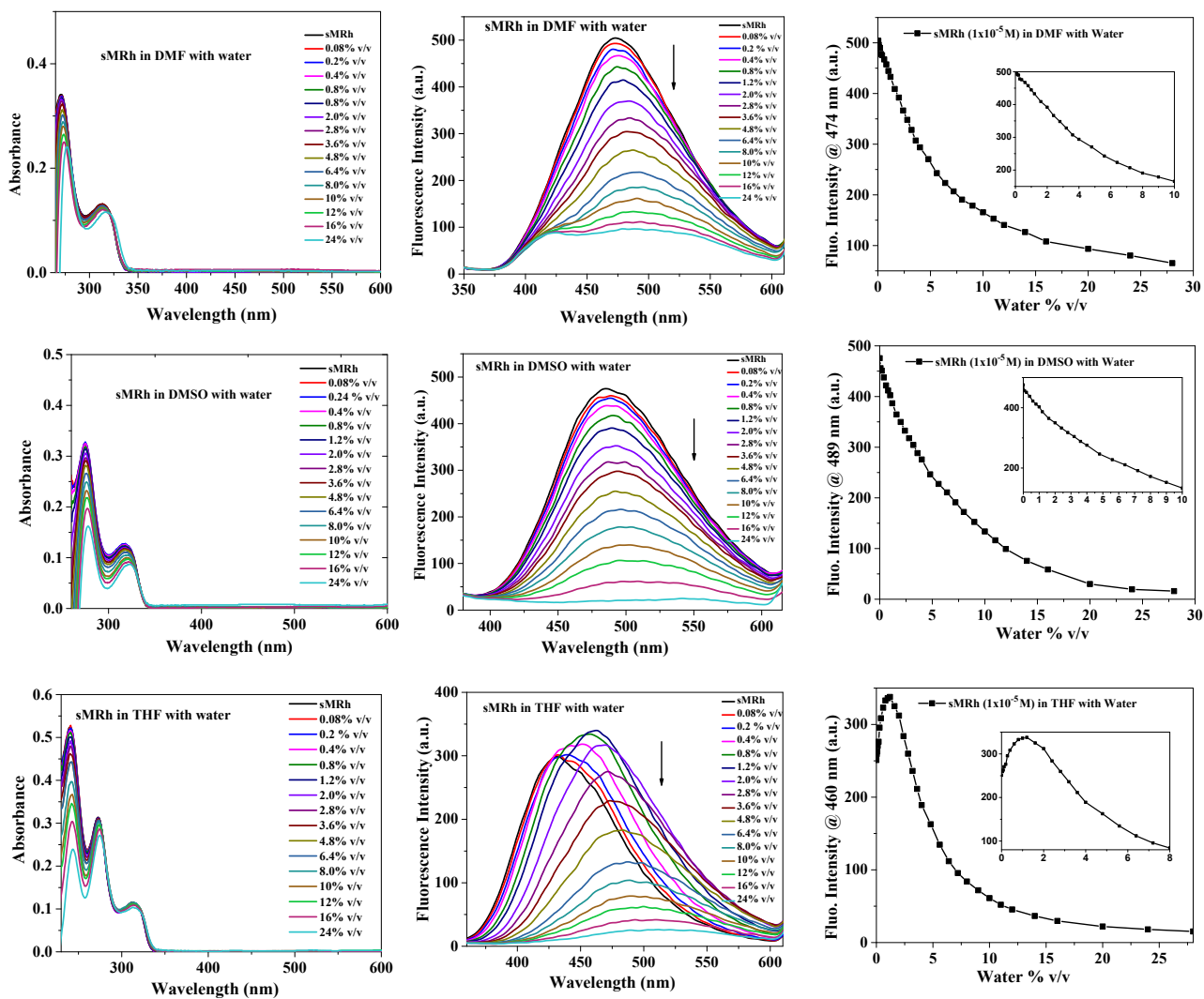


Figure S10. Fluorescence spectrum and fluorescence emission intensity of the sMRh as a function of the water content in DMF, DMSO and THF.

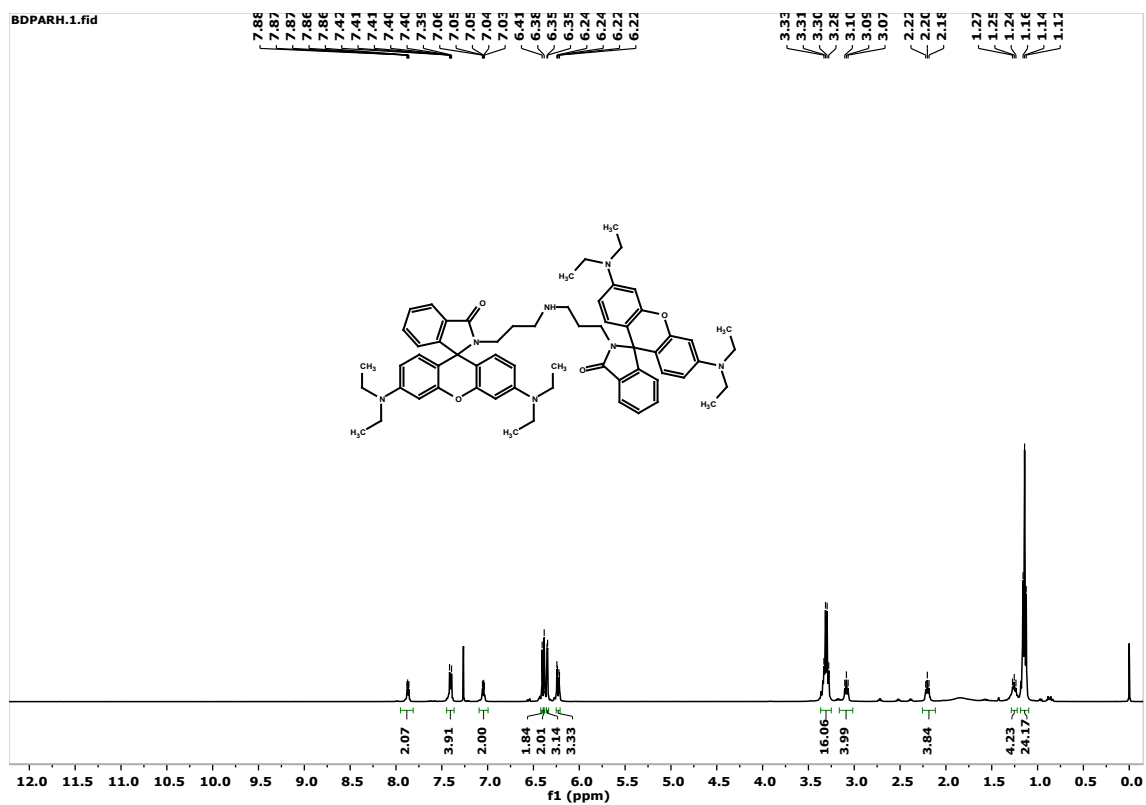


Figure S11. ^1H NMR spectrum of sDRh in CDCl_3

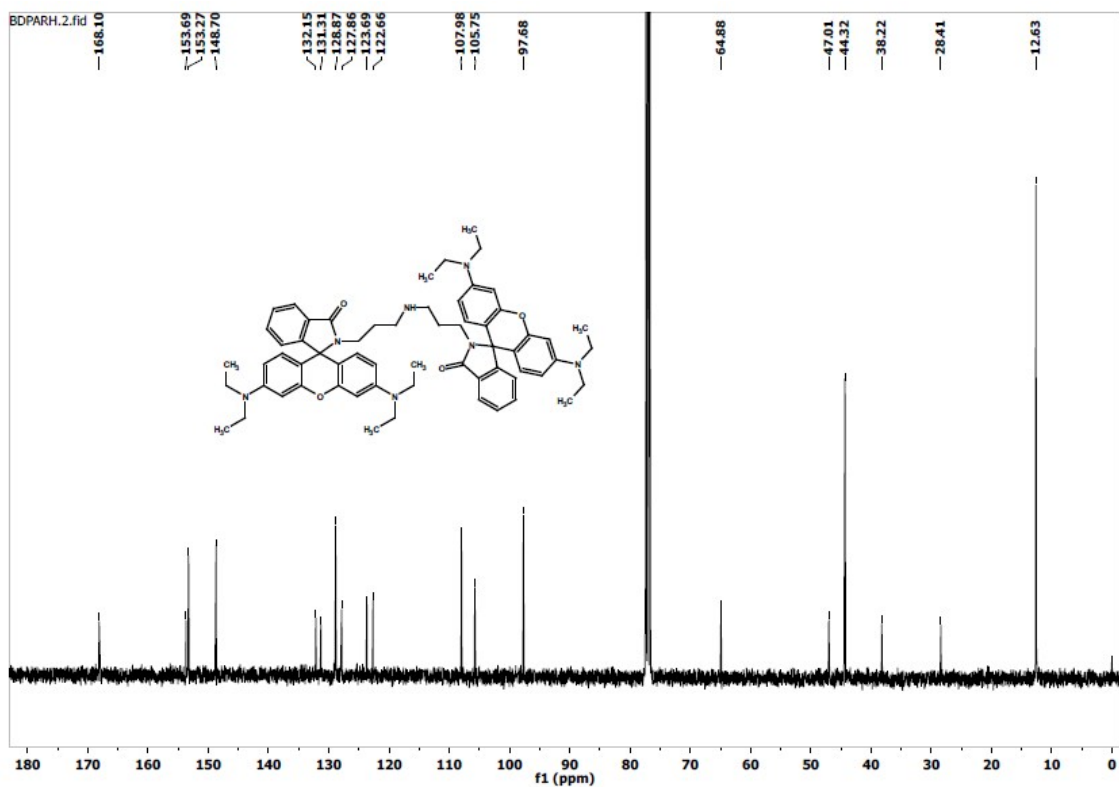


Figure S12. ^{13}C NMR spectrum of sDRh in CDCl_3

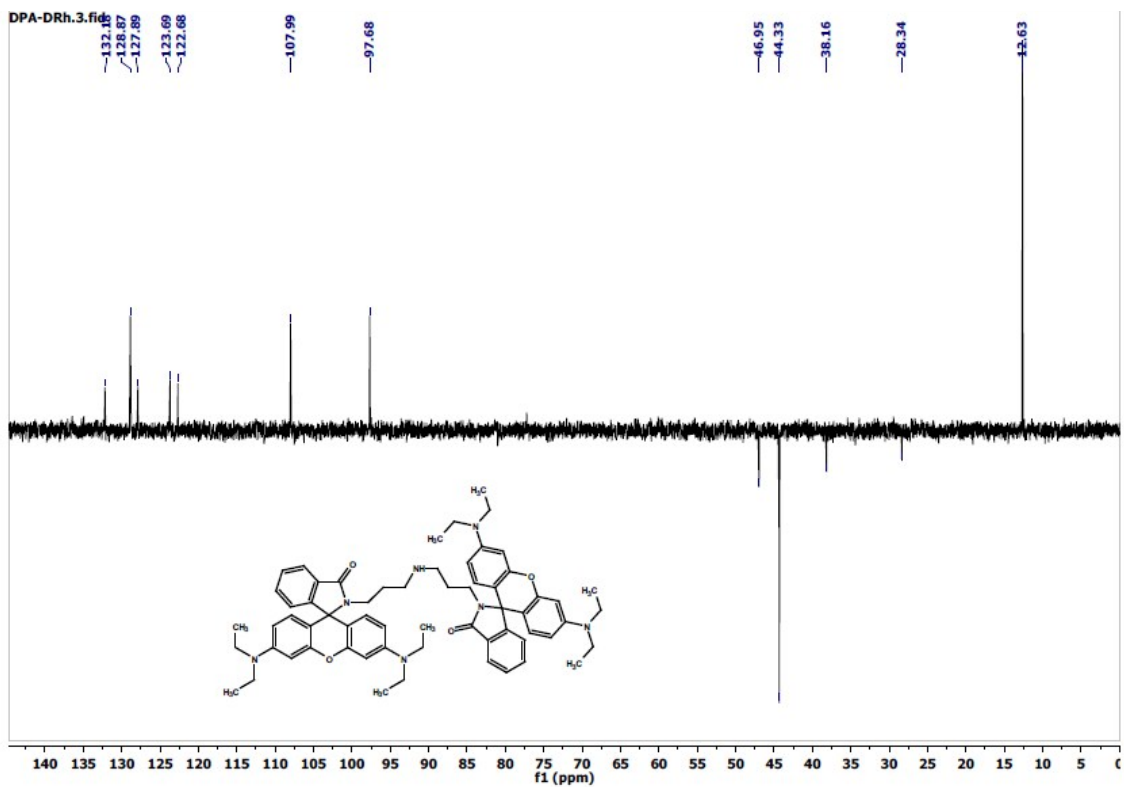


Figure S13. DEPT 135 ^{13}C NMR spectrum of sDRh in CDCl_3

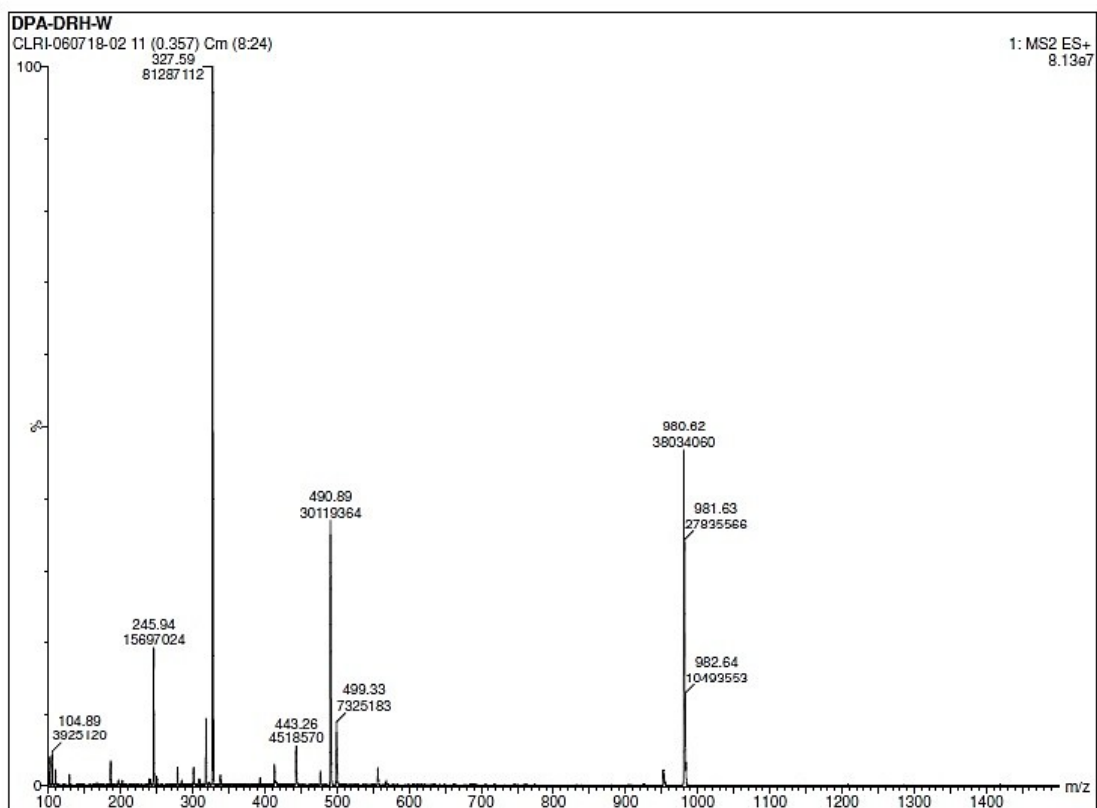


Figure S14. ESI-MS spectrum of sDRh

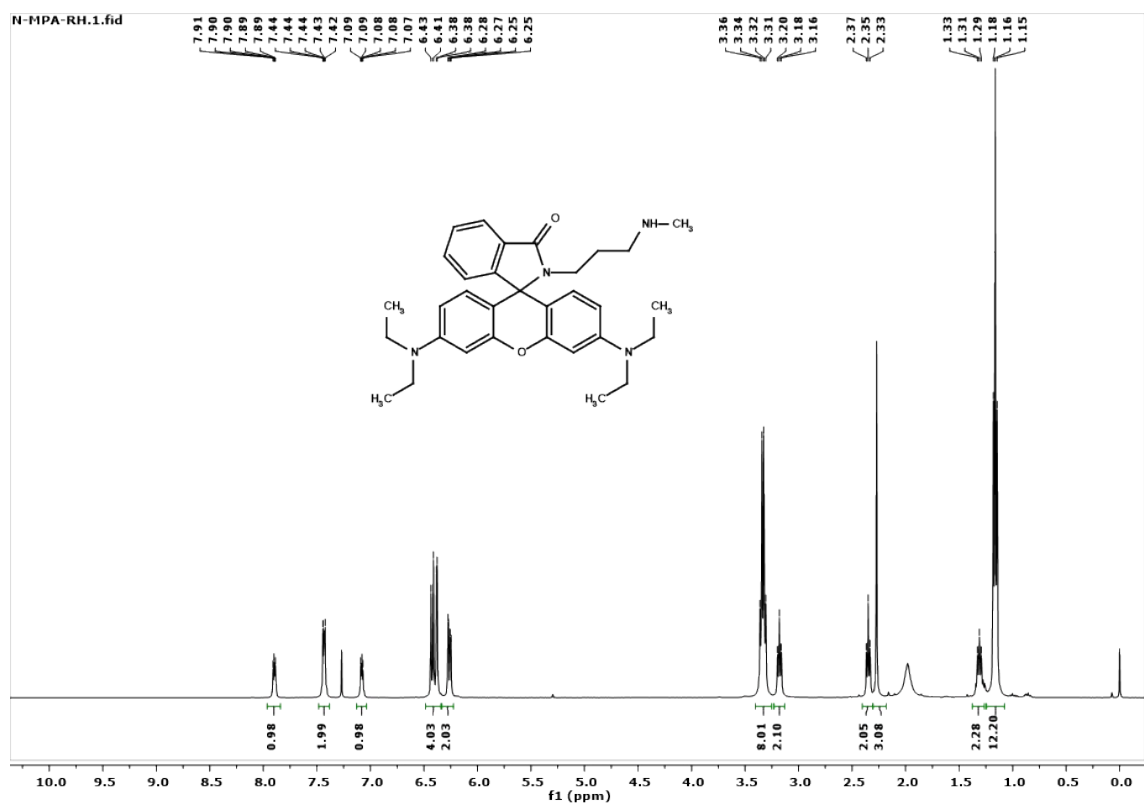


Figure S15. ^1H NMR spectrum of sMRh in CDCl_3

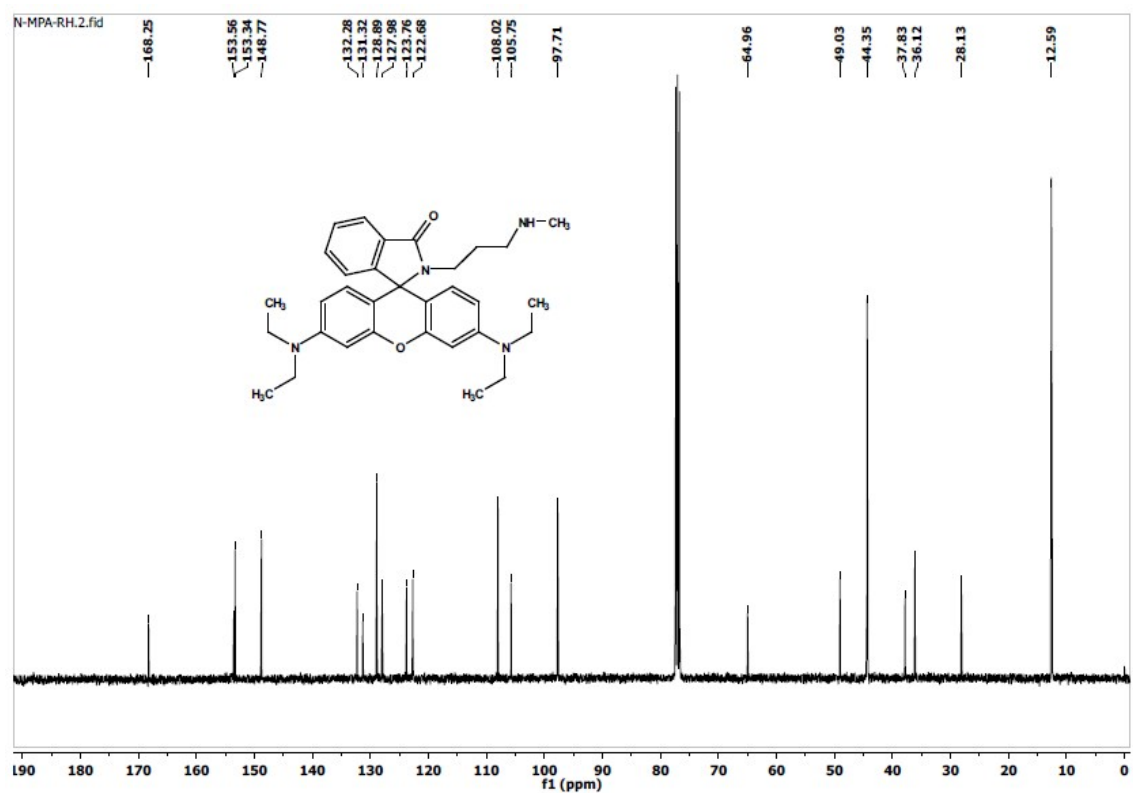


Figure S16. ^{13}C NMR spectrum of sMRh in CDCl_3

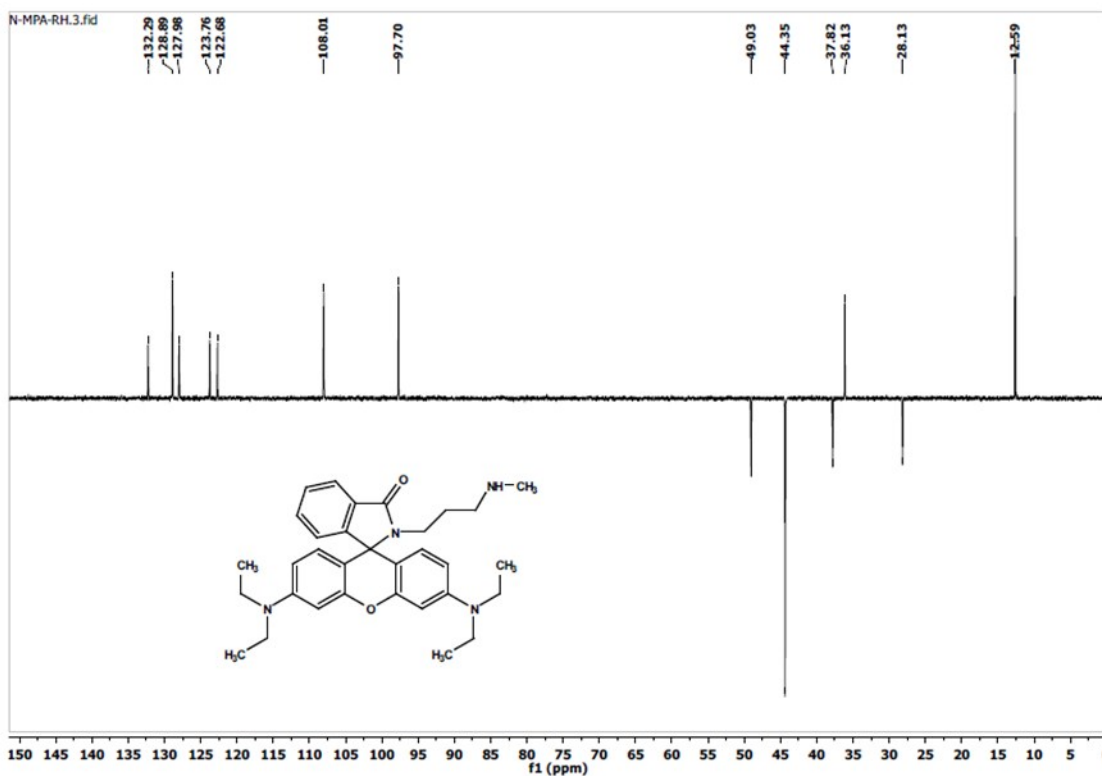


Figure S17. DEPT 135 ^{13}C NMR spectrum of sDRh in CDCl_3

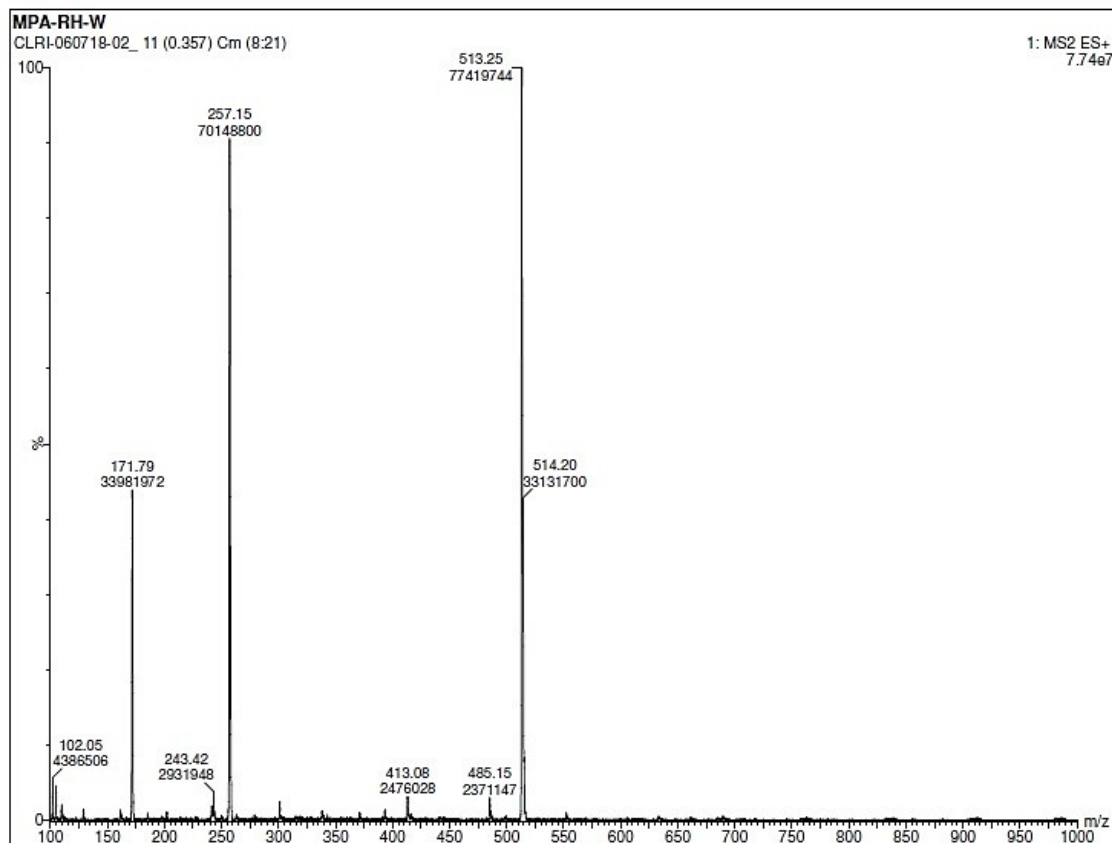


Figure S18. ESI-MS spectrum of sDRh

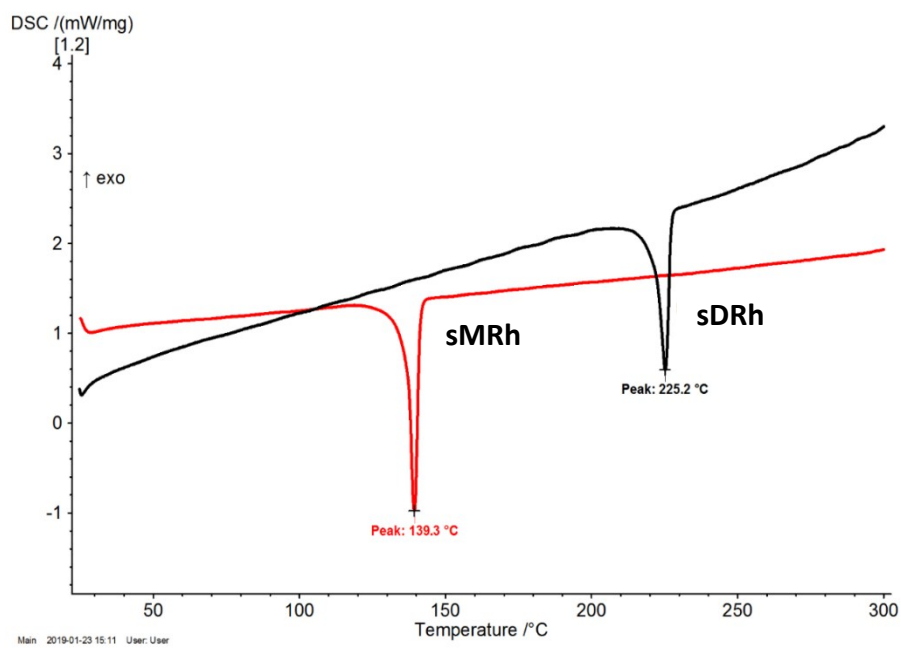


Figure S19. Differential Scanning Calorimetry of sDRh and sMRh

References

1. Y. Kubota, Y. Sakuma, K. Funabiki and M. Matsui, *The Journal of Physical Chemistry A*, 2014, **118**, 8717-8729.